Dissecting the Order of Bacteriophage T4 DNA Polymerase Holoenzyme Assembly†

Daniel J. Sexton,‡ Barbara Fenn Kaboord,§ Anthony J. Berdis, Theodore E. Carver,|| and Stephen J. Benkovic*

Department of Chemistry, 152 Davey Laboratory, The Pennsylvania State University, University Park, Pennsylvania 16802

Received January 12, 1998; Revised Manuscript Received March 23, 1998

ABSTRACT: Most biological organisms rely upon a DNA polymerase holoenzyme for processive DNA replication. The bacteriophage T4 DNA polymerase holoenzyme is composed of the polymerase enzyme and a clamp protein (the 45 protein), which functions as a processivity factor by strengthening the interaction between DNA and the holoenzyme. The 45 protein must be loaded onto DNA by a clamp loader ATPase complex (the 44/62 complex). In this paper, the order of events leading to holoenzyme formation is investigated using a combination of rapid-quench and stopped-flow fluorescence spectroscopy kinetic methods. A rapid-quench strand displacement assay in which the order of holoenzyme component addition is varied provided data indicating that the rate-limiting step in holoenzyme assembly is associated with the clamp loading process. Pre-steady-state analysis of the clamp loader ATPase activity demonstrated that the four bound ATP molecules are hydrolyzed stepwise during the clamp loading process in groups of two. Clamp loading was examined with stopped-flow fluorescence spectroscopy from the perspective of the clamp itself, using a site-specific, fluorescently labeled 45 protein. A mechanism for T4 DNA polymerase holoenzyme assembly is proposed in which the 45 protein interacts with the 44/62 complex leading to the hydrolysis of 2 equiv of ATP, and upon contacting DNA, the remaining two ATP molecules bound to the 44/62 complex are hydrolyzed. Once all four ATP molecules are hydrolyzed, the 45 protein is poised on DNA for association with the polymerase to form the holoenzyme.

Processive DNA synthesis is required for the efficient replication of genomic DNA. To achieve processive DNA synthesis, the DNA polymerase may associate with a processivity factor, such as a sliding clamp protein, to form a holoenzyme complex. This sliding clamp tethers the polymerase to the DNA, thereby strengthening the interaction between the holoenzyme and DNA during replication. The X-ray crystallographic structure of the sliding clamp from yeast (PCNA), *Escherichia coli* (β-clamp), and bacteriophage T4 (the gene 45 protein) has been solved (*1*,*2*; personal communication, John Kuriyan). Despite a lack of sequence homology and deviations in quaternary structure (the β-clamp is a dimer while PCNA and the 45 protein are trimers), they all possess a similar ring-like structural motif with approximately equivalent dimensions (*3, 4*). The ring shape suggests that the source of the enhanced holoenzyme stability on DNA is mediated by a topological link between the DNA and the clamp. The clamp is loaded onto DNA by a clamp loader protein complex. Clamp loaders from eukaryotes, *E. coli*, and bacteriophage T4 have been characterized as multiprotein complexes that require ATP hydrolysis for functional holoenzyme formation (*5*−*8*). The mechanism of loading the clamp onto DNA is not understood in depth despite contributions from several laboratories (*9*−*13*).

The bacteriophage T4 DNA replication system is well suited for detailed mechanistic investigations due to a minimal protein complement that retains functions found in higher organisms (*14*−*16*). The T4 holoenzyme is composed of the polymerase (gene 43 protein) and the gene 45 protein, which is loaded onto DNA by the T4 clamp loader (gene 44/62 protein complex). The 45 protein is also involved in the transcriptional activation of late T4 genes (*17*). The 44/62 complex is comprised of a ratio of four 44 subunits to one 62 subunit (*8*). It has been shown that the 44/62 complex loads the 45 protein onto DNA in a catalytic manner through the hydrolysis of four bound ATP molecules (*9, 13, 18*).

Recently, a site-specific, fluorescently labeled 45 protein was found to provide further insight into the role of ATP hydrolysis in holoenzyme assembly (*19*). This fluorescent assay for holoenzyme assembly is unique in that it monitors interactions from the perspective of a sliding clamp protein. By monitoring changes in the steady-state fluorescence of the labeled 45 protein, events in holoenzyme assembly were assigned as either dependent upon or independent of ATP hydrolysis. Remarkably similar fluorescence changes were reported using a different fluorescent probe attached at a different site on the 45 protein (*20*). The fluorescence data were in agreement with DNA footprinting (*21*) and protein−DNA cross-linking experiments in that ATP binding without hydrolysis was found sufficient for the formation of a 44/62 complex-mediated 45 protein−DNA interaction (*22*). ATP hydrolysis, however, was required to observe by cryoelectron microscopy stable structures on nicked DNA that corresponded to bound 45 protein (*23*) and to generate a DNA polymerase holoenzyme capable of strand displacement synthesis (*9, 19*).

†This work was supported by National Institutes of Health Grants GM13306 (S.J.B.), GM15729 (T.E.C.), GM16704 (A.J.B.), and GM15239 (B.F.K.).

* To whom correspondence should be addressed. Tel, (814) 865-2882; fax, (814) 865-2973; e-mail: sjb1@psu.edu.

‡ Present address: Dyax Corp., One Kendall Square, Building 600, Cambridge, MA 02139.

§ Present address: Pharmacia Biotech Inc., 202 North Bartlett Ave., Milwaukee, WI 53202.

|| Present address: Argonne National Laboratory, Argonne, IL 60439.

S0006-2960(98)00088-9 CCC: $15.00
Published on Web 05/06/1998

Despite previous reports that provided hints into the order of holoenzyme assembly, the detailed order of molecular events has not been established (*7, 11, 18*). In the T4 system, rapid kinetic studies have shown that the rate-limiting step for holoenzyme assembly is approximately 1 s^{-1} (*18*). Though the exact identity of this step has not yet been determined, its similarity to the pre-steady-state rate for ATPase activity suggests that ATP hydrolysis is either associated with the rate-limiting step or is preceded by the rate-limiting step (*9*).

In this paper, a variety of rapid kinetic techniques were utilized to investigate the order of T4 DNA polymerase holoenzyme assembly. A rapid-quench strand displacement assay demonstrated that the clamp loading process is the overall rate-limiting step in T4 DNA polymerase holoenzyme assembly. The pre-steady-state ATPase kinetic parameters of the 45•44/62 complex were reevaluated in the presence or absence of DNA. A detailed investigation of the individual events within the clamp loading process was then performed using the fluorescently labeled analogue of the 45 protein (*19*) in combination with stopped-flow fluorescence spectroscopy. The data collectively provide a kinetic sequence for holoenzyme formation.

EXPERIMENTAL PROCEDURES

Materials. Oligonucleotides were synthesized with an Expedite 8909 DNA synthesizer (Perceptive Biosystems), deprotected according to the protocol supplied by the manufacturer and gel purified according to Capson et al. (*24*). 3′-Biotin-labeled oligonucleotides were prepared using a BioTEG CPG column as obtained from Glen Research. The fluorescent probe *N*-((2-iodoacetoxy)ethyl-*N*-methyl)amino-7-nitrobenz-2-oxa-1,3-diazole (IANBD) was obtained from Molecular Probes. ATP-γ-S was purchased from Boehringer Mannheim as a 98% pure solution and used without further purification. New England Nuclear was the source of the [α-^{32}P]dCTP and the [γ-^{32}P]ATP used to 5′-end label oligonucleotides with T4 polynucleotide kinase (United States Biochemical). All other biochemicals and chemicals were obtained from either Sigma or Fisher Scientific and were of analytical grade or better.

Protein Preparations. The wild-type 45 protein and the 44/62 complex were purified as previously described (*25, 26*) from *E. coli* transformed with expression vectors obtained from Dr. William Konigsberg (Yale University). The T7C-45 protein was purified in the same manner but was expressed in *E. coli* from a pET expression vector obtained from Dr. John Kuriyan (Rockefeller University). The preparation of the IANBD-labeled T7C mutant of the 45 protein was previously reported (*19*). The concentration of the 45 protein is expressed in terms of the trimer, and the concentration of the 44/62 complex reflects a stoichiometry of four 44 subunits to one 62 protein. The T4 exonuclease-deficient polymerase D219A mutant was purified as published (*27*) and used in all of the following experiments to avoid complications arising from the presence of the exonuclease activity. The polymerase activity of the T4 D219A polymerase is identical to that of the wild-type enzyme (*27*).

Primer Template Construction. The biotinylated 34/62/36mer DNA substrate was constructed as previously described (*28*). This DNA substrate is composed of a 34mer primer annealed to a 3′-biotinylated 62mer with a 36mer fork strand annealed to the 5′-end of the template to leave a 5′-18 base overhang. Quantitation of this primer/template was achieved by a Klenow fragment [α-^{32}P]dCTP incorporation procedure (*24*).

Steady-State Fluorescence. Steady-state fluorescence measurements were performed using an SLM Aminco 8000C photon-counting spectrofluorometer equipped with a thermostated cell compartment maintained at 25 °C. Excitation and emission slit widths were each maintained at 4 nm. The obtained fluorescence spectra were normalized for the effects of dilution.

Stopped-Flow Fluorescence. Stopped-flow fluorescence measurements were performed using an Applied Photophysics stopped-flow instrument at a constant temperature of 25 °C. The excitation wavelength was 475 nm, and the excitation slit widths were 2.4 nm. The changes in fluorescence were observed upon stopped-flow mixing of syringe A and syringe B. The syringe contents for each experiment are as described in the accompanying figure legends or table footnotes.

Strand Displacement Assay. A rapid-quench strand displacement assay was utilized to assay the effect of varying the order of holoenzyme component addition on the rate of formation of active holoenzyme (*28, 29*). The mixing time between two different protein−DNA solutions was varied (from 0.1 to 60 s) before the addition of dNTPs and single-strand DNA trap. Polymerization proceeded for 10 s before being acid quenched (0.3 M HCl final) and neutralized with an appropriate amount of 3 M NaOH in 1 M Tris base. Samples were extracted with phenol:chloroform:isoamyl alcohol extraction (25:24:1) and loaded onto a 16% polyacrylamide/8 M urea sequencing gel. The sequencing gels were exposed to constant current electrophoresis, and the distribution of the radioactivity was analyzed using a Molecular Dynamics phosphorimager.

Pre-Steady-State ATPase Assay. The pre-steady-state ATPase rates were measured using a KinTek rapid-quench instrument (*9, 29*). The assay mixture composition is described in the legend to Table 2. The reactions were quenched with 1 M HCl and neutralized with an appropriate amount of 3 M NaOH in 1 M Tris base prior to product separation by thin-layer chromatography and analysis with a Molecular Dynamics phosphorimager.

Data Analysis. Kinetic data were fit to one of the following equations using the curve-fitting software included in the Kaleidograph program:

single exponential: $$y = Ae^{-kt} + C \quad (1)$$

single exponential with linear phase: $$y = Ae^{-kt} + Bt + C \quad (2)$$

double exponential: $$y = Ae^{-kt} + A_2e^{-k_2t} + C \quad (3)$$

second-order function when reactant concentrations are equal: $$y = D/((Dk't) + 1) + C \quad (4)$$

second-order function when reactant concentrations are neither equal nor in excess of the other: $$\ln[(X_t - D_{1o})/(X_t - D_{2o})] = k't(D_{2o} - D_{1o}) + C \quad (5)$$

where A is the amplitude of the exponential phase, k is the exponential rate constant, B is the linear rate constant, D is the concentration of reactants, D_{1o} is the starting concentra-

Scheme 1

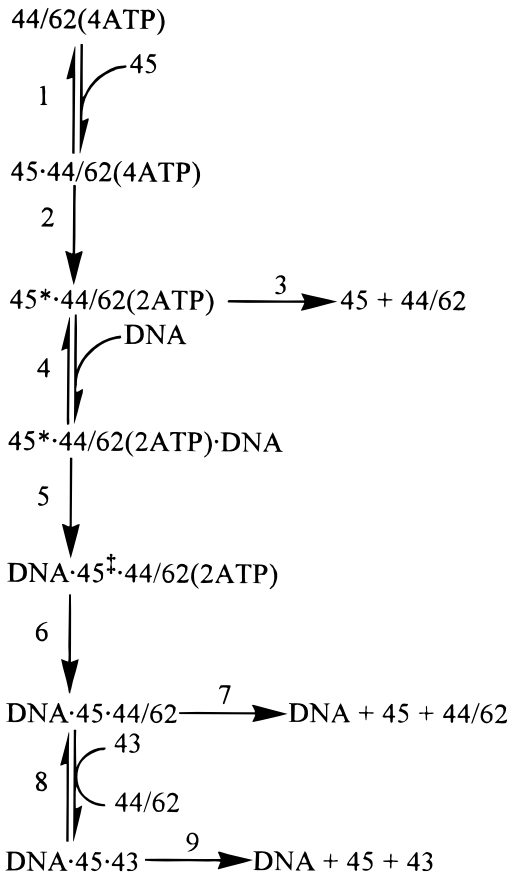

tion of one reactant, D_{2o} is the starting concentration of the other reactant, X_t is the product concentration at time t, k' is the second-order rate constant, and C is an offset.

Simulation of Holoenzyme Assembly. The stopped-flow fluorescence data were simulated using the PC version of the KinSim program (*30*) with the mechanism shown in Scheme 1 and the parameters listed in Table 4 (see Discussion).

RESULTS

Effect of Order of Addition on Holoenzyme Assembly. The overall rate-limiting step in T4 DNA polymerase holoenzyme assembly was investigated by varying the order of addition of the holoenzyme components. Complex formation was monitored by measuring the amount of strand displacement synthesis that occurred on a biotinylated, forked 34/62/36mer DNA substrate (*18*). Approximately the same rate constant for holoenzyme assembly ($1-2$ s^{-1}) was observed for all the conditions listed in Table 1 except when the 45 protein was preincubated with the DNA, the 44/62 complex, and ATP prior to introduction of the T4 polymerase. In this case, the rate for holoenzyme assembly increased to approximately 60 s^{-1}.

Pre-Steady-State ATPase Analysis of the 45·44/62 Complex. It had been previously demonstrated by kinetic analysis that ATP hydrolysis by the 45·44/62 complex is biphasic (*9, 13*). The initial burst phase represents the pre-steady-state whereas the slower phase corresponds to the steady-state hydrolysis of ATP. In the presence of DNA, the burst amplitude signified that all four molecules of ATP bound to the 44/62 complex were hydrolyzed (*9*). In the absence of DNA, the observed burst amplitude corresponded to hydrolysis of only two of the four ATP sites on the 44/62 complex (Figure 1). The observed ATPase pre-steady-state rate (5 ± 2 s^{-1}; Figure 1) was slightly faster than in the presence of DNA ($\sim$1 s^{-1}; *9*). The steady-state ATPase rates also differed at 110 ± 10 nM/s in the absence of DNA and 200 ± 10 nM/s in the presence of DNA (*9*).

Table 1: Effect of the Order of Addition on the Rate of Complex Assembly[a]

syringe A	syringe B	$k_{complex}$ (s^{-1})
DNA + ATP	43 + 44/62 + 45	1.2 ± 0.1
DNA + 44/62 + ATP	43 + 45	1.3 ± 0.1
DNA + 44/62 +45 + ATP	43	64 ± 4
DNA + 45 + 43	44/62 +ATP	2.3 ± 0.4
DNA + 43	44/62 + 45 + ATP	2.7 ± 0.2

[a] Strand displacement assays were performed as described in the Materials and Methods section and as developed by Kaboord and Benkovic (*18*). The assay mixtures contained 500 nM DNA (Bio34/62/36mer), 550 nM streptavidin, 100 nM T4 polymerase (43 protein), 550 nM 45 protein, 550 nM 44/62 complex, 1 mM ATP, 10 μM dNTPs, 1 mg/mL single strand salmon sperm DNA trap, and an ATP regenerating system (3 mM phospoenolpyruvate and 6 U/mL pyruvate kinase) in complex buffer (20 mM Tris, pH 7.5, 150 mM potassium acetate, 10 mM magnesium acetate, 10 mM β-mercaptoethanol, and 1 mM EDTA). Rate constants were extracted from a fit to a single-exponential equation (eq 1).

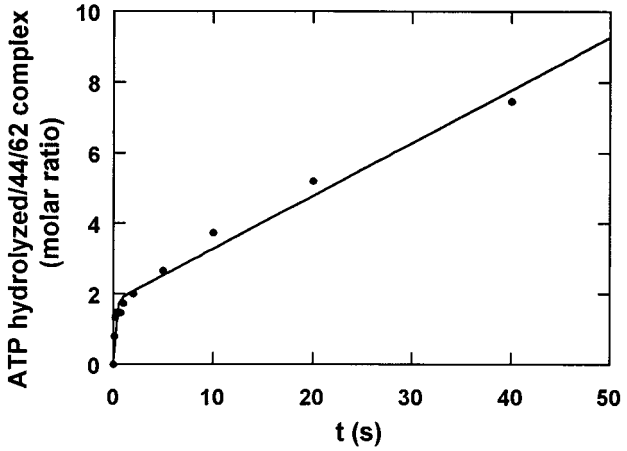

FIGURE 1: Pre-steady-state ATP hydrolysis by the 45·44/62 complex. ATP hydrolysis by the 44/62 complex (750 nM) was observed in the presence of the 750 nM 45 protein and 1 mM [γ-^{32}P]-ATP in complex buffer as described in the Materials and Methods section. The following parameters were extracted from a fit to eq 3: burst amplitude = 1.5 ± 0.2 μM; pre-steady-state rate = 5 ± 2 s^{-1}; and steady-state rate = 110 ± 10 nM/s.

Dissection of Holoenzyme Formation Using Stopped-Flow Fluorescence Spectroscopy. A series of experiments were initiated in order to define the minimal kinetic sequence and the magnitude of the associated rate constants leading to the holoenzyme. The initial set focused on the interactions between the 45 and 44/62 proteins in the presence of ATP or ATP-γ-S, while the second set considered 44/62 complex mediated interactions of the 45 protein with DNA.

Formation of a 45·44/62 Complex. The lack of cysteine residues in the 45 protein was previously exploited for the site-specific introduction of a fluorescent probe (*19*). A cysteine mutant of the 45 protein (T7C-45 protein) was labeled via cysteine thiol alkylation with the environmentally sensitive fluorescent probe, IANBD. This fluorescent protein (T7C-45-ANBD) possessed unaltered function yet produced

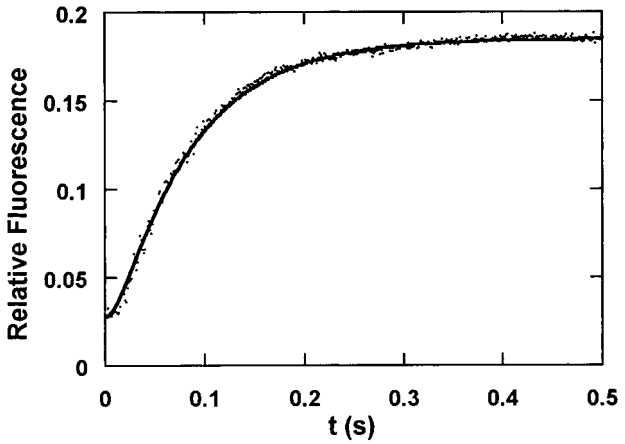

FIGURE 2: Formation of an ATP hydrolysis dependent 45·44/62 complex. The ATP hydrolysis dependent interaction of the T7C-45-ANDB protein (250 nM) with the 44/62 protein (2 μM) and 1 mM ATP in complex buffer was monitored using stopped-flow fluorescence spectroscopy with an excitation wavelength of 475 nm. The data (circles) were well fit by a single exponential (eq 1) (Table 2) and simulated by steps 1−3 of Scheme 1 using the parameters from Table 4 (solid line).

substantial changes in probe fluorescence intensity upon interacting with other components necessary for the formation of the holoenzyme. The T7C-45-ANBD protein interacts with the 44/62 complex to produce a stoichiometric species of increased fluorescence intensity (designated as the 45*·44/62 complex). The formation of this species requires ATP hydrolysis, as it was not observed upon substitution of ATP with the nonhydrolyzable ATP analogue, ATP-γ-S (*19*).

The rate of 45*·44/62 complex formation was monitored by stopped-flow fluorescence spectroscopy (Figure 2). Mixing low or equal concentrations of the 44/62 complex and the T7C-45-ANBD protein in the presence of ATP provided the second-order rate constant for formation of the presumed, initial 45·44/62·ATP complex (Table 2, row 1). When the T7C-45-ANBD protein was mixed with a molar excess of the 44/62 complex and ATP, the resulting time-dependent fluorescence change was best approximated by a single-exponential kinetic process (Figure 2; Table 2, row 2). The reaction order of this fluorescence change was investigated by holding one component (either the 45 protein or the 44/62 complex) constant at 250 nM and varying the concentration of the other up to either 2 μM 44/62 complex or 8 μM 45 protein (data not shown). Under these conditions, increasing the concentration of the limiting component did not lead to an additional rate enhancement, suggesting that the fluorescence change is limited by a conformational change in the 45·44/62 complex.

Dissociation of the 45·44/62 Complex. The decay of the highly fluorescent, ATP hydrolysis dependent 45*·44/62 complex was monitored by mixing the preformed complex with a substance capable of either consuming or preventing hydrolysis of subsequent molecules of ATP. A solution containing equal amounts of T7C-45-ANBD protein, 44/62 complex, and excess ATP was mixed against either EDTA or a glucose/hexokinase cocktail to consume available ATP. Irrespective of the manner in which ATP was removed, the dissociation of this 45·44/62 complex was best approximated by a single-exponential decay with a fluorescence amplitude (Table 2, row 3) that matched the increase in fluorescence observed in Table 2, rows 1 and 2. The first-order kinetic nature of this dissociation process was confirmed upon observing approximately the same rate constant with a 2-fold increase in the protein concentration (data not shown).

Formation of the 45·DNA Complex. The remaining experiments focus on conformational changes in the 45 protein induced by binding to DNA. The change in fluorescence that was observed when the T7C-45-ANBD protein interacted with DNA (*19*) was analyzed by stopped-flow fluorescence spectroscopy. The highly fluorescent 45*·44/62 complex was mixed against DNA to produce an observed net decrease in fluorescence that was approximated by a double-exponential process (Figure 3). The amplitude of this decay is consistent with the expected decrease in fluorescence intensity that would occur upon interaction of the highly fluorescent 45*·44/62 complex with DNA (*19*). The initial exponential decay was assigned an observed rate constant of approximately 30 s^{-1} (Figure 3; Table 3, row 1). Following this fluorescence decrease, there was an increase in fluorescence that exhibited an observed rate constant of about 1 s^{-1}. The first-order nature of these processes was established by their insensitivity to increasing the DNA concentration above 500 nM and subsequent doubling of the 45*·44/62 complex concentration (data not shown).

Formation of an ATP Hydrolysis Independent 45·44/62·DNA Complex. The 45 protein and the 44/62 complex have been previously implicated to form a complex using the nonhydrolyzable ATP analogue, ATP-γ-S (*19, 22*). A fluorescence change was observed upon interaction of T7C-45-ANBD·44/62·ATP-γ-S complex with DNA (*19*). The magnitude of this fluorescent increase was consistent with the formation of a species where the T7C-45-ANBD protein is associated with DNA.

The time dependence of this fluorescence change was investigated using stopped-flow fluorescence spectroscopy in order to assign observed rate constants. Stopped-flow mixing of DNA against a T7C-45-ANBD·44/62·ATP-γ-S complex produced an observed rate constant of 2.1 ± 0.1 s^{-1} (Table 3, row 2). Varying the DNA concentration (125−500 nM) produced similar rate constants (data not shown).

Dissociation of the 45·44/62·DNA Complex. It was possible to monitor the dissociation of the 45 protein from DNA by adding EDTA to the solution (Figure 4; Table 3, row 3). It was not feasible to use the glucose/hexokinase system to measure the holoenzyme dissociation rate constant (*19*) because the time required for this system to deplete the ATP was not sufficiently short. EDTA blocks ATP hydrolysis by chelating the required magnesium ions. The usefulness of EDTA in determining complex dissociation constants was established by the finding that it provided the same holoenzyme dissociation rate constant (0.01 s^{-1}) as that reported using the glucose/hexokinase system (data not shown; *19*). Mixing the ATP-dependent 45·44/62·DNA complex against EDTA resulted in a fluorescence decay that was best approximated by a function incorporating a single exponential (1 s^{-1}) and a linear rate constant (1 nM/s), which may be due to a small amount of protein precipitation during the assay time course. (Figure 4; Table 3, row 3).

DISCUSSION

In this paper, reenforcing sets of pre-steady-state kinetic methods were used to investigate processes associated with

Table 2: Summary of the Clamp·Clamp Loader Interaction Kinetic Parameters[a]

row	syringe A	syringe B	k_{obs}	fluorescence amplitude[b]	assembly step[c]
1	45	44/62 + 1 mM ATP	$31 \pm 16\ \mu M^{-1}\ s^{-1}$ [d]	na[e]	1
2	250 nM 45	2 μM 44/62 + 1 mM ATP	$14 \pm 1.4\ s^{-1}$	$+0.18 \pm 0.01$	2
3	250 nM 45 + 250 nM 44/62 + 1 mM ATP	50 mM EDTA	$0.35 \pm 0.02\ s^{-1}$	-0.19 ± 0.01	3

[a] Note that the above concentrations were 2-fold more concentrated in the syringe prior to mixing in the presence of complex buffer. All rate constants were obtained by a fit to a single-exponential equation (eq 1), except that shown in row 1, which was derived from a second order equation with the assumption that the observed fluorescence amplitude was directly proportional to product concentration (eq 4 or 5). In all cases the observed rate constants were obtained with stopped-flow fluorescence using the T7C-45-ANBD protein. [b] A positive amplitude signifies a fluorescence increase whereas a negative amplitude signifies a fluorescence decrease. [c] This designation refers to the holoenzyme assembly mechanism (Scheme 1) and is described in the Discussion section. [d] This average rate constant was obtained using 250 nM T7C-45-ANBD protein and varied 44/62 concentrations (25, 62.5, 125, 250 nM). Under stoichiometric conditions (250 nM each), the data were fit to eq 4; whereas, when the 44/62 complex was substoichiometric, eq 5 was used to fit the data. [e] Not applicable; fluorescence values were converted to units of concentration using the specific fluorescence value for the labeled 45 protein ($0.11\ \mu M^{-1}$) and that of the 45*·44/62 complex ($0.78\ \mu M^{-1}$).

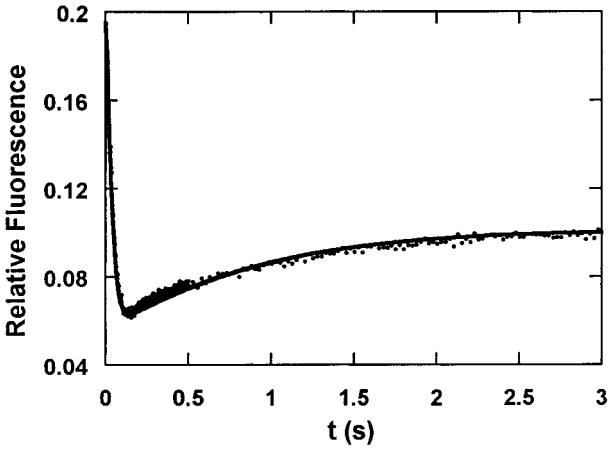

FIGURE 3: Formation of the 45·DNA complex. The consequence of T7C-45-ANDB protein interaction with DNA was monitored using stopped-flow fluorescence. A solution containing 500 nM T7C-45-ANDB protein, 500 nM 44/62 complex, and 2 mM ATP was mixed against a DNA (1 μM Bio34/62/36mer with 1.1 μM streptavidin) solution. The above concentrations were diluted 2-fold upon mixing, and all solutions were prepared in complex buffer. The data (circles) were fit by a single exponential (eq 1) (Table 3) and simulated by Scheme 1 using the parameters from Table 4 (solid line).

T4 DNA polymerase holoenzyme assembly. Information reflecting the overall assembly rate for the entire holoenzyme complex was acquired from a rapid-quench strand displacement assay. The rate constants obtained using that assay preclude observation of individual events within holoenzyme assembly. Measurements of the pre-steady-state ATPase activity of the clamp loader complex provided kinetic parameters to be assigned to steps involving ATP hydrolysis. Stopped-flow fluorescence spectroscopy employing a fluorescently labeled clamp protein revealed further details of the holoenzyme assembly process. The labeled 45 protein was well suited for reporting intramolecular conformational transitions but unable to report directly protein−protein or protein−DNA encounters. The combination of kinetic approaches employed in this paper has led to the construction of a minimal kinetic mechanism for holoenzyme assembly (Scheme 1). In the following discussion, the rationale dictating the design of Scheme 1 is documented. Support for the proposed holoenzyme assembly mechanism was obtained by kinetic simulation of the data to Scheme 1 using the parameters listed in Table 4.

Clamp Loading is the Rate-Limiting Step in Holoenzyme Assembly. Initially, we sought to assess quantitatively the contribution of the clamp loading process to the overall rate of complex assembly. The rate-limiting process was investigated by measuring the effect of varying the order of holoenzyme component addition on the rate of holoenzyme assembly (Table 1). It is immediately apparent from Table 1 that the assembly rate was greatest when the 45 protein was apparently preloaded onto DNA by the 44/62 complex prior to introduction of the polymerase (step 8 of Scheme 1). Therefore, the rate-limiting step must be attributed to an event(s) before step 8 involving 45 protein loading onto DNA. Step 8 was written as an interaction between the polymerase and a 45·44/62·DNA complex based on a previous finding that the 44/62 complex has chaperone activity with respect to polymerase holoenzyme association (*18*).

Formation of a 45·44/62 Complex (Steps 1−3). Scheme 1 begins with the 44/62 complex already bound to ATP, as it was previously demonstrated that addition of ATP facilitates the interaction of the 44/62 complex with both DNA and the 45 protein (*21, 22*). However, it has been shown that in the absence of ATP a distinct complex is formed between the 45 protein and the 44/62 protein (*31*). The process by which the 44/62 complex binds ATP was not analyzed, but von Hippel and co-workers were able to investigate this early event in holoenzyme assembly and found that the 44/62 complex binds four molecules of ATP with a K_d of 34 μM (*13*).

The interaction of the 45 protein with the 44/62 complex was examined using a fluorescently labeled 45 protein (T7C-45-ANBD protein). This fluorescent protein exhibits an ATP hydrolysis dependent fluorescence increase upon interaction with the 44/62 complex (*19*). At the concentrations of the 45 protein used in these studies, a substantial amount of this protein is predicted to exist as a monomer, rather than the functionally competent trimer (*32*). The finding that the yeast clamp loader does not recognize its clamp monomers (*33*) suggests that the same result would be observed in T4. However, it was previously shown that the T7C-45-ANBD protein interacts stoichiometrically with the 44/62 complex in the presence of ATP even at concentrations where more than half of the 45 protein is in its monomeric form (*19*). This observation implies that the 44/62 complex assembles the 45 protein into its active trimeric form.

The T7C-45-ANBD protein was used to demonstrate by stopped-flow fluorescence that the interaction between the ATP-bound 44/62 complex and the 45 protein occurs through a bimolecular process (step 1), followed by a unimolecular process that is dependent upon ATP hydrolysis (step 2). Step

Table 3: Summary of Clamp·DNA Interaction Kinetic Parameters[a]

row	syringe A	syringe B	k_{obs}	fluorescence amplitude[b]	assembly step[c]
1	45 + 44/62 + ATP	DNA	$30 \pm 2\ s^{-1}$	-0.13 ± 0.01	5
			$1 \pm 0.3\ s^{-1}$	$+0.05 \pm 0.001$	6
2	45 + 44/62 + ATP-γ-S	DNA	$2 \pm 0.1\ s^{-1}$	$+0.13 \pm 0.01$	not shown
3	45 + 44/62 + ATP + DNA	EDTA	$1 \pm 0.2\ s^{-1}$	-0.08 ± 0.01	7
			1 ± 0.4 nM/s		

[a] The final concentrations (after mixing) of the T7C-45-ANBD protein and the 44/62 complex was 250 nM in complex buffer for rows 1−4 and 500 nM in row 5. The final concentration of DNA (Bio34/62/36mer) was 500 nM in the presence of 550 nM streptavidin while ATP or ATP-γ-S was diluted to 1 mM. In all cases, observed rate constants were obtained by stopped flow fluorescence using the T7C-45-ANBD protein. [b] A positive amplitude signifies a fluorescence increase whereas a negative amplitude signifies a fluorescence decrease. [c] This designation refers to the holoenzyme assembly mechanism (Scheme 1) as described in the Discussion section.

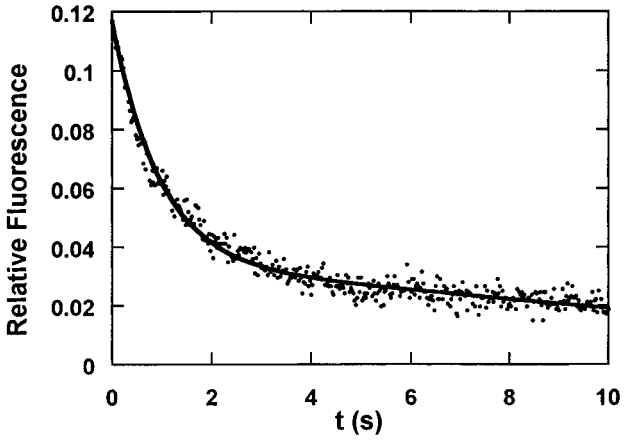

FIGURE 4: Dissociation of the 45·DNA complex. The dissociation of the T7C-45-ANDB protein from DNA was monitored using stopped-flow fluorescence. A solution containing 500 nM T7C-45-ANDB protein, 500 nM 44/62 complex, 2 mM ATP DNA, 1 μM Bio34/62/36mer, and 1.1 μM streptavidin in complex buffer was pushed against 100 mM EDTA in complex buffer minus the magnesium acetate. The above concentrations were diluted 2-fold upon mixing. The data (circles) were fit by a single exponential followed by a steady state (eq 2) (Table 3).

2 of Scheme 1 was assigned as being an ATP hydrolysis dependent first-order kinetic process, which likely reflects a conformational change in the 45 protein (45*·44/62 species). This conformational changed may be tied to opening the 45 protein ring prior to loading onto DNA. The 45*·44/62 species undergoes an exponential decay upon removal of available ATP (step 3; Table 2). This off rate matches the previously determined steady-state ATPase rate (*9*), which suggests that steady-state ATP hydrolysis by the 45·44/62 complex is limited by protein dissociation. The ratio of the apparent rate constants for the formation (k_1) and dissociation (k_3) of the 45*·44/62 complex is very similar to the apparent K_d value (8 nM) reported by Latham et al. (*20*) and observed in our lab (12 nM, D.J.S. and S.J.B., unpublished observations). Therefore, this apparent K_d is comprised of more than one kinetic step.

The interaction between the 45 protein and the 44/62 complex in the presence of ATP was modeled using steps 1−3 of Scheme 1 and the parameters listed in Table 4 (Figure 2). The data were fit by setting the experimentally determined rate constants for step 2 ($14\ s^{-1}$) and step 3 ($0.35\ s^{-1}$) as fixed values and varying the forward ($k_{forward}$) and reverse rate constants ($k_{reverse}$) associated with step 1. The data could be simulated using a wide range of values for $k_{forward}$ and $k_{reverse}$ provided that their ratio was approximately constant, which predicts a dissociation constant of about 400 nM for the interaction between the 45 protein and the 44/62 complex prior to ATP hydrolysis (Table 4). As with all the simulations preformed in this study, the intermediate concentrations were converted to fluorescence by multiplying the concentrations by the specific fluorescence values shown in Table 4.

ATP Hydrolysis Coupled 45·44/62 Formation.* The 44/62 complex hydrolyzes ATP to load the 45 protein onto DNA such that a pre-steady-state burst of ATP hydrolysis is followed by a steady-state ATPase rate (*9*). The observation of burst kinetic behavior indicates that the chemical hydrolysis step is not the rate-limiting step in ATP turnover by the 44/62 complex (*33*). It is known that the 44/62 complex is composed of a 4:1 ratio of 44 proteins to 62, with the ATPase activity residing on each of the 44 proteins (*25*). In the presence of DNA, the 45·44/62(4ATP) complex exhibited a burst amplitude corresponding to stoichiometric ATP hydrolysis by all four 44 sites of the 44/62 complex (*9*).

It was therefore surprising to observe that in the absence of DNA the burst amplitude was consistent with the hydrolysis of only two molecules of ATP per 45·44/62-(4ATP) complex (Figure 1). Since all four subunits were previously shown to hydrolyze ATP during the clamp loading process (*9*, *13*), these data suggest that all four ATP molecules are not hydrolyzed simultaneously. The binding of ATP is noncooperative, effectively excluding the possibility of sequential binding events (*13*). Consequently, ATP hydrolysis may proceed stepwise in sets of two through a 45·44/62(2ATP) intermediate, where the second set can only be hydrolyzed once the accessory protein complex interacts with DNA. The initial hydrolysis event may be associated with opening the ring of the clamp protein.

The acid quench of the assay releases all products (ADP and P_i) bound at the active site, so all the hydrolyzed ATP is accountable. Attempts to measure accurately the pre-steady-state rate for ATP hydrolysis associated with the first set were thwarted by sensitivity limitations in the early time interval. Values for the ATPase pre-steady-state rate constant vary from 1 to $15\ s^{-1}$ (*9*, *13*), which overlaps that measured by stopped-flow fluorescence for the conformational change in the 45 protein (Table 2, row 2).

The 45 Protein·DNA Interaction (Steps 4−6). Loading the 45 protein onto DNA by the 44/62 complex was examined using the fluorescently labeled T7C-45-ANBD protein. The steady-state fluorescence intensity of the T7C-45-ANBD protein was previously shown to be sensitive to interaction with DNA (*19*). This fluorescence change was now used to examine kinetic parameters dependent upon the interaction of the 45 protein with DNA.

Table 4: Holoenzyme Assembly Simulation Parameters

step[a]	species$_{initial}$	$F'_{initial}$ (μM^{-1})		species$_{final}$	F'_{final} (μM^{-1})	$k_{forward}$	K_D
1	45 + 44/62	0.11[b]	⇄	45·44/62	0.11	*c*	0.3−0.5 μM[c]
2	45·44/62	0.11	→	45*·44/62	0.78	14 s^{-1}	*d*
3	45*·44/62	0.78	→	45 + 44/62	0.11	0.35 s^{-1}	*d*
4	45*·44/62 + DNA	0.78	⇄	45*·44/62·DNA	0.78	*e*	∼0.05 μM[e]
5	45*·44/62·DNA	0.78	→	DNA·45‡·44/62	0.23	40−60 s^{-1}	*d*
6	DNA·45‡·44/62	0.23	→	DNA·45·44/62	0.6	0.5−0.7 s^{-1}	*d*
7	DNA·45·44/62	0.6	→	DNA + 45 + 44/62	0.11	0.3−0.6 s^{-1}	*d*

[a] This designation refers to the holoenzyme assembly mechanism (Scheme 1) as described in the Discussion section. [b] $F'_{initial}$ refers to the specific fluorescence of the fluorescent species of 45 protein present initially, whereas F'_{finals} refers to the specific fluorescence after the indicated interaction or conformational change. $F'_{initial}$ was calculated for the free 45 protein by dividing the initial fluorescence by the total 45 protein concentration. The specific fluorescence of the highly fluorescent species (45*·44/62 and 45*·44/62·DNA) was calculated by dividing its observed total fluorescence by its concentration. The specific fluorescence of the DNA·45‡·44/62 and DNA·45·44/62 intermediates was set based on their observed fluorescence and predicted concentrations. [c] The forward rate constant is not shown, but it could vary in the simulation between 30 and 80 μM^{-1} s^{-1} with complementary reverse rate constants from about 10 to 40 s^{-1} to yield an apparent K_d between 0.3 and 0.5 μM. [d] Assumed irreversible. [e] In order to fit the data in Figure 3, the forward rate constant for this step had to be 100 μM^{-1} s^{-1} with a reverse rate constant of about 5 s^{-1} to yield an apparent K_d of 0.05 μM. The apparent error in these parameters is approximately 10−20%.

Mixing the preformed highly fluorescent 45*·44/62·(2ATP) complex with DNA led to an initial complex (45*·44/62·(2ATP)·DNA) of unchanged fluorescence (step 4) that subsequently displayed a fluorescence decay followed by a fluorescence increase to an intermediate level (Figure 3). These data were simulated using Scheme 1 and the rate constants and specific fluorescence values previously assigned to Figure 2. Maintaining the parameters from the previous simulation (Figure 2) allowed fewer parameters to float during the simulation of the data in Figure 3 to Scheme 1. The interaction of the 45*·44/62(2ATP) complex with DNA (step 4) appears to occur with an apparent K_d of about 0.05 μM (Table 4). It is evident from Table 4 that differences exist between the experimentally determined observed rate constants (Table 3) and the predicted intrinsic rate constants for steps 5−7. However, the good simulation of Figure 3 to Scheme 1 supports the proposed order of holoenzyme assembly. Although this order of assembly rationalizes the kinetic observations, alternative pathways may exist due to the number of components involved and the inability of the T7C-45-AND protein to provide clear protein−protein and protein−DNA signals.

The inability of the probe to report directly the association of the 45*·44/62(2ATP) complex and DNA is consistent with the notion that the 44/62 complex chaperones the 45 protein to DNA. The subsequent fast step (step 5) may be a conformational change in the 45*·44/62(2ATP)·DNA complex that results in the direct interaction of the fluorescently labeled 45 protein with DNA [indicated as DNA·45*·44/62(2ATP) in Scheme 1]. The second slower conformational change (step 6) is very similar to the reported rate-limiting step for holoenzyme assembly (*28*). Furthermore, its similarity to the previously reported pre-steady-state ATPase rate constant measured in the presence of DNA (*9*) suggests that this step may involve the hydrolysis of the remaining two molecules of ATP. It is tempting to speculate that this slow conformational change in the 45 protein (step 12) may represent the closing of the 45 protein around DNA.

The dependence of the interaction of the 45·44/62 complex with DNA on ATP hydrolysis was investigated by substituting ATP with ATP-γ-S. The fluorescence change observed using ATP-γ-S is also attributed to a conformational change in the 45·44/62 complex on DNA, although it occurs much slower than in the presence of ATP (2 vs 30 s^{-1}). In the absence of ATP hydrolysis, it appears that the 45·44/62 complex first associates with DNA in a fluorescently silent manner and then undergoes a distinct conformational change.

Dissociation of the 45·DNA Complex (Step 7). The dissociation of the 45 protein from DNA has been implicated as being much faster than analogous clamp proteins from yeast and *E. coli (35, 36)*. The relatively fast dissociation of the 45 protein from may suggest an altered solution conformation of the 45 protein, especially while on DNA. Prior to this study, the direct measurement of the dissociation of the 45 protein from DNA had not been accomplished.

Efficient lagging strand DNA synthesis is believed to require the recycling of the DNA polymerase holoenzyme from a completed Okazaki fragment to a freshly synthesized primer. This reutilization of the holoenzyme components requires the efficient dissociation of both the polymerase and the clamp protein. Holoenzyme disassembly during lagging strand synthesis involves an accelerated simultaneous dissociation of both the polymerase and the clamp components (*37, 38*). The observed holoenzyme dissociation rate constant was enhanced from about 0.003−0.01 s^{-1} for the paused holoenzyme (step 9; *19, 28, 39*) to about 0.3 s^{-1} for the holoenzyme after extension on a DNA substrate that simulates lagging strand synthesis (*37*).

The present study showed that the 45 protein rapidly dissociates from DNA with an observed rate constant of about 1 s^{-1} (step 7; Table 3). The exact identity of the observed species of the 45 protein that dissociates from the DNA is not known. The 45 protein may dissociate from DNA with the 44/62 protein pair or as a single entity (i.e., not in a complex with the 44/62 protein). The simulated 45·DNA off rate constant was about 0.3 s^{-1}, which is very similar to the observed dissociation rate constant of the holoenzyme upon encountering a previous Okazaki fragment (*37*). It is possible that the previous Okazaki fragment triggers rapid holoenzyme dissociation by disabling the interaction between the T4 polymerase and clamp such that they dissociate from DNA independently. In *E. coli*, the clamp loader has been implicated in the dissociation of the clamp protein from DNA (*11*). In contrast, the relatively fast k_{off} of the 45 protein from DNA makes a 44/62 catalyzed dissociation event unnecessary. Indeed, no evidence for the 44/62 complex-catalyzed DNA dissociation of the 45 protein has been observed.

Summary. A consideration of the kinetic characteristics of holenzyme formation from the perspective of holoenzyme-dependent polymerization, clamp loader ATPase activity, and observable protein−protein and protein−DNA interactions has provided insight into the order of holoenzyme assembly. The proposed assembly mechanism follows a pathway where the 45 protein interacts first with the 44/62 complex and hydrolyzes 2 equiv of ATP. The resulting 45*·44/62 complex contacts DNA and hydrolyzes the remaining two bound ATP molecules before the polymerase is introduced into the complex. The rate-limiting step in holoenzyme assembly appears to be coupled to a conformational change in the 45 polymerase on DNA. Exit from this kinetic bottleneck leaves the 45 protein poised on DNA for rapid association with the polymerase (step 8). Rigorous proof for this pathway will require additional experimentation.

REFERENCES

1. Kong, X.-P., Onrust, R., O'Donnell, M., and Kuriyan, J. (1992) *Cell 69*, 425−437.
2. Krishna, T. S. R., Kong, X.-P., Gary, S., Burgers, P. M., and Kuriyan, J. (1994) *Cell 79*, 1233−1243.
3. Kelman, Z., and O'Donnell, M. (1995) *Annu. Rev. Biochem. 64*, 171−200.
4. Kuriyan, J., and O'Donnell, M. (1993) *J. Mol. Biol. 234*, 915−925.
5. Dallmann, H. G., and McHenry, C. S. (1995) *J. Biol. Chem. 270*, 29563−29569.
6. Gary, S. L., and Burgers, P. M. J. (1995) *Nucleic Acids Res. 23*, 4986−4991.
7. Onrust, R., Finkelstein, J., Naktinis, V., Turner, J., Fang, L., and O'Donnell, M. (1995) *J. Biol. Chem. 270*, 13348−13357.
8. Jarvis, T. C., Paul, L. S., and von Hippel, P. H (1989) *J. Biol. Chem. 264*, 12709−12716.
9. Berdis, A. J., and Benkovic, S. J. (1996) *Biochemistry 35*, 9253−9265.
10. Bloom, L. B., Turner, J., Kelman, Z., Beechem, J. M., O'Donnell, M., and Goodman, M. F. (1996) *J. Biol. Chem. 271*, 30699−30708.
11. Naktinis, V., Onrust, R., Fang, L., O'Donnell, M. (1995) *J. Biol. Chem. 270*, 13358−13365.
12. Podust, L. M., Podust, V. N., Sogo, J. M., and Hubscher, U. (1995) *Mol. Cell. Biol. 15*, 3072−3081.
13. Young, M. C., Weitzel, S. E., and von Hippel, P. H. (1996) *J. Mol. Biol. 264*, 440−452.
14. Nossal, N. G. (1992) *FASEB J. 6*, 871−878.
15. Young, M. C., Reddy, M. K., and von Hippel, P. H. (1992) *Biochemistry 31*, 8675−8690.
16. Sexton, D. J., Berdis, A. J., and Benkovic, S. J. (1997) *Curr. Opin. Chem. Biol. 1*, 316−322.
17. Herendeen, D. R., Kassavetis, G. A., and Geiduschek, E. P. (1992) *Science 256*, 1298−1303.
18. Kaboord, B. F., and Benkovic, S. J. (1996) *Biochemistry 35*, 1084−1092.
19. Sexton, D. J., Carver, T. E., Berdis, A. J., and Benkovic, S. J. (1996) *J. Biol. Chem. 271*, 28045−28051.
20. Latham, G. J., Pietroni, P., Dong, F., Young, M. C., and von Hippel, P. H. (1996) *J. Mol. Biol. 264*, 426−439.
21. Munn, M. M., and Alberts, B. M. (1991) *J. Biol. Chem. 266*, 20020−20033.
22. Capson, T. L., Benkovic, S. J., and Nossal, N. G. (1991) *Cell 65*, 249−258.
23. Gogel, E. P., Young, M. C., Kubasek, W. L., Jarvis, T. C., and von Hippel, P. H. (1992) *J. Mol. Biol. 224*, 395−412.
24. Capson, T. L., Peliska, J. A., Kaboord, B. F., Frey, M. W., Lively, C., Dahlberg, M., and Benkovic, S. J. (1992) *Biochemistry 31*, 10984−10994.
25. Nossal, N. G. (1979) *J. Biol. Chem. 254*, 6026−6031.
26. Rush, J., Lin, T.-C., Quinones, M., Spicer, E. K., Douglas, I., Williams, K. R., and Konigsberg, W. H. (1989) *J. Biol. Chem. 264*, 10943−10953.
27. Frey, M. W., Nossal, N. G., Capson, T. L., and Benkovic, S. J. (1993) *Proc. Natl. Acad. Sci. U.S.A. 90*, 2579−2583.
28. Kaboord, B. F., and Benkovic, S. J. (1995) *Curr. Biol. 5*, 149−157.
29. Johnson, K. A. (1986) *Methods Enzymol. 134*, 677−705.
30. Frieden, C. (1994) *Methods Enzymol. 240*, 311−322.
31. Pietroni, P., Young, M. C., Latham, G. J., and von Hippel, P. H. (1997) *J. Biol. Chem. 272*, 31666−31676.
32. Soumillion, P., Sexton, D. J., and Benkovic, S. J. (1998) *Biochemistry 37*, 1819−1827.
33. Jonsson, Z. O., Podust, V. N., Podust, L. M., and Hubsher, U. (1995) *EMBO J. 14*, 5745−5751.
34. Fersht, A. (1985) *Enzyme Structure and Mechanism*, 2nd ed., W. H. Freeman and Co., New York.
35. Fu, T.-J., Sanders, G. M., O'Donnell, M., and Geiduschek, E. P. (1996) *EMBO J. 15*, 4414−4422.
36. Yao, N., Turner, J., Kelman, Z., Stukenberg, P. T., Pan, Z.-Q., Hurwitz, J., and O'Donnell, M. (1996) *Genes Cells 1*, 101−113.
37. Carver, T. E., Sexton, D. J., and Benkovic, S. J. (1997) *Biochemistry 36*, 14409−14417.
38. Hacker, K. J., and Alberts, B. M. (1994) *J. Biol. Chem. 269*, 24221−24228.
39. Hacker, K. J., and Alberts, B. M. (1994) *J. Biol. Chem. 269*, 24209−24220.

BI980088H